Effect of the substrate dilution on the room and high temperature tribological behaviour of Ni-based coatings deposited by PTA on grey cast iron

F. Fernandes, T. Polcar, A. Loureiro, A. Cavaleiro

PII: S0257-8972(15)30272-3
DOI: doi: 10.1016/j.surfcoat.2015.09.034
Reference: SCT 20585

To appear in: *Surface & Coatings Technology*

Received date: 30 April 2015
Revised date: 18 September 2015
Accepted date: 19 September 2015

Please cite this article as: F. Fernandes, T. Polcar, A. Loureiro, A. Cavaleiro, Effect of the substrate dilution on the room and high temperature tribological behaviour of Ni-based coatings deposited by PTA on grey cast iron, *Surface & Coatings Technology* (2015), doi: 10.1016/j.surfcoat.2015.09.034

Effect of the substrate dilution on the room and high temperature tribological behaviour of Ni-based coatings deposited by PTA on grey cast iron

F. Fernandes[1,*],T. Polcar[2,3], A. Loureiro[1], A. Cavaleiro[1]

[1]CEMUC - Department of Mechanical Engineering, University of Coimbra, Rua Luís Reis Santos, 3030-788 Coimbra, Portugal.

[2]Department of Control Engineering Czech Technical University in Prague Technicka 2, Prague 6, 166 27 Czech Republic.

[3]n-CATS University of Southampton Highfield Campus SO17 1BJ Southampton, UK.

[*]Email address: filipe.fernandes@dem.uc.pt, tel. + (351) 239 790 745, fax. + (351) 239 790 701

Abstract

In the present investigation the effect of the substrate dilution on room and high temperature (550 and 700 ºC) tribological behaviour of nickel based hardfaced coating deposited by plasma transferred arc onto a grey cast iron was investigated and compared to the uncoated grey cast iron. At room temperature, the wear loss of coatings was independent of the substrate dilution and similar to the grey cast iron. At high temperatures, coating produced with high dilution displayed the highest wear resistance between all the samples. This is attributed to the formation of a protective tribo-layer resulting from the agglomeration of a high amount of oxide debris due to its lower oxidation resistance when compared to the sample produced with low dilution.

Keywords: Plasma transferred arc, Ni-based alloy, Substrate dilution effect, Tribology, High temperature wear

1. Introduction

Cast irons and copper-alloys are commonly used in the production of glass molds and accessories for glass industry, owing to their excellent thermal conductivity and relatively low cost [1]. Molds are often exposed to severe conditions of abrasion, oxidation, wear, fatigue at high temperature, due to repeated contact with melted glass, causing deformation or failure of parts and, thus, compromising the product quality and increasing the maintenance costs. To overcome this shortcoming, protective coatings are normally applied in some zones of molds surfaces with the aim of increasing their lifetime in harsh environments [2, 3]. A wide diversity of coating materials have been successfully applied to protect the surface of these components, such as: cobalt, iron and nickel alloys [2, 4, 5]. The latter have been especially used due to their outstanding performance under extreme high temperature conditions [5-8]. Several hardfacing and thermal spraying processes have been used to coat the molds: (i) plasma transferred arc (PTA) and gas tungsten arc welding (GTAW), (ii) flame spraying (FS), high velocity oxy fuel (HVOF) and atmospheric plasma spraying (APS). Hardfacing processes have been preferentially used in the protection of mold surfaces because they promote a strong metallurgical bonding between the coating and the substrate, condition required to achieve high quality adherent coatings and to avoid the catastrophic failure in service, as opposed to thermal spraying processes where only a mechanical bonding is established. Among the hardfacing processes referred to above, PTA has been widely used to protect the surface of molds, since it produces high quality thick coatings,

offering both optimal protection with minimal thermal distortion of parts and high deposition rates in single layer deposits [4, 5]. However, the properties and the quality of deposits are strongly dependent on the dilution of the substrate promoted by the PTA process. Low dilution provides coatings with similar chemical composition to the added metal powder, condition for achieving enhanced mechanical properties, wear and oxidation resistance [9]. To avoid adhesion problems and, therefore, not to compromise the performance of molds in service, it is common to increase the dilution through the change of the most relevant deposition parameters even if the mechanical properties, wear and oxidation resistance are diminished. In our previous studies [10-12] the effect of increasing dilution, promoted by change of arc current on the structure, mechanical properties, oxidation resistance and wear behaviour of a nickel-based alloy deposited onto a grey cast iron have been investigated. Regarding the wear behaviour of coatings, it was evaluated at room temperature in a ball cratering wear tester. However, none studies concerning the tribological performance of such coatings at high temperature have been conducted. Hence, as a way to complement the previous works, the aim of this investigation is to study the effect of increasing substrate dilution on the tribological performance at room and essentially at high temperature of Ni-based coating deposited onto grey cast iron, using a pin on disc tribometer apparatus. Comparison of these results with those achieved for the base material used in molds production, which is also in contact with the melted glass in the uncoated zones, is also provided.

2. Experimental procedure

A nickel-based hardfacing alloy powder named Colmonoy 215 (from Colmonoy company) was deposited by plasma transferred arc using a Commersald Group ROBO

90 machine onto flat surfaces of grey cast iron blocks, currently used in the production of molds for the glass industry. Two different arc currents (100 and 140 amperes) were used on the depositions to produce coatings with two dissimilar levels of dilution. Hereinafter, the coatings deposited using 100 and 140 amperes will be denominated as C100 and C140, respectively. Table 1 gives the optimized parameters used in the depositions, while Table 2 depicts the nominal chemical composition of the base material and Colmonoy 215 powder. Before coating, the substrate blocks were preheated at 480 ºC to reduce the heating rate and, therefore, to avoid the susceptibility to cracking during deposition. Using the same deposition conditions, several weld beads, each with approximately 3 to 5 mm thick, were deposited in parallel on the cast iron, ensuring some overlapping between them in order to obtain a 35×35 mm coated surface area and a quasi-flat surface. Specimens containing cast iron and coating were removed from each block for microstructural and micro-hardness analysis. Further, specimens with dimension of 20×20×5 mm were removed from each block for tribological testing. The coated surfaces were first machined to provide flatness and then grinded and polished following standard procedures to obtain a uniform roughness of about 0.51 – 0.62 µm.

The tribological behaviour of the coatings and grey cast iron was evaluated at room and high temperatures using a pin-on-disk tribometer. This is a well-known and worldwide recognized technique that has been used as a standard to evaluate the tribological behaviour of a wide range of materials and coatings at high temperature. As the operating surface temperature of moulds is currently in the range of 500 - 900 ºC, temperatures of 550 and 700 ºC were selected to perform the experiments. Although in the real working conditions of molds, glass is the main responsible for the molds wear, due to its melted state at high temperature, for the tribological tests we have selected as

counterpart a harder and more resistant material: Al_2O_3 balls. Thus, we ensure that the wear volume loss of coatings will be overestimated in relation to the expected loss in actual service conditions. All the wear tests were conducted at a constant linear speed of 0.10 $m.s^{-1}$, a load of 5 N, a relative humidity of 48±5%, and 5000 cycles. The radius of the wear tracks was set to 5.3 mm. Such parameters were selected in order to produce wear tracks with measurable volume loss and to avoid the formation of very high contact areas between the sphere and the tested material. During the tests, the friction coefficient was continuously recorded. In order to ensure the reproducibility of the results, two tests were performed under identical conditions for each coating. The average of the wear rate and associated error was obtained through 6 measurements (3 per sample), performed at different zones (bottom, left and upper part) of the wear track. The specimens tested at high temperature were heated from room temperature (RT) up to the desired temperature at a linear ramp of 30 ºC/min. After reaching the testing temperature, 10 min holding time was allowed for ensuring an evenly distribution of temperatures on the specimen. After tests, the specimens were cooled down with air blowing with an approximately cooling rate of ~ 20ºC/min. The wear rate of the coatings was determined through the analysis of the wear track using a 3D optical profilometer. Wear tracks and wear debris were characterized by scanning electron microscopy with energy dispersive X-ray spectroscopy (SEM-EDS) and by Raman spectroscopy. The Raman spectra were acquired using HORIBA Jobin-Yvon Raman device with visible light source with a wavelength of 532 nm. The spectra were measured in the range 100 - 2000 cm^{-1} with a laser power of 20 or 25 mW; acquisition time was 30s. All measurements were performed at room temperature.

3. Results and discussion

Prior to the tribological tests, a short overview about the main characteristics of the coatings investigated within this work is provided, based on our previous papers [10-12]. The typical microstructure of the coatings produced with 100 and 140 A is exemplified in Fig. 1. Both coatings display relatively dense microstructure with excellent adhesion to the substrate, free of microcracks and with only a few solidification pores. Their typical microstructure consists of primary dendrites of a (Ni, Fe) face centred cubic solid solution phase aligned along the direction of heat flow, with the occurrence of N_3Si, Cr_5B_3 and Fe_3Mo_3C phases. Moreover, other precipitates such as C-B and Mo-C were also identified in the grain boundaries by WDS analysis. The dendritic structure became finer as the arc current increased due to the higher amount of precipitates formed on the grain boundaries. Flakes of carbon (dark-floret like phase) randomly distributed in the matrix can be also perceived, being more notorious on C140 coating, in good agreement with the increase of dilution promoted by the higher arc current. Following the procedure described in reference [11], dilutions of ~28 and ~59% were measured for C100 and C140 coatings, respectively. The dilution is beneficial in terms of improving the adhesion, but it can bring some disadvantages, such as change in the hardness and chemical composition, and lowering of wear and oxidation resistance of the coatings [9]. The chemical composition of the coatings, assessed by SEM-EDS, is given in Table 3. The measurements were performed in area (400×400 μm) on the center of the cross section of each coating; 3 measurements were performed in each sample. This procedure was used to ensure that the chemical composition was determined in a representative volume of material in that zone, thus avoiding the problems that punctual analyses can give rise in heterogeneous materials. The results

show that the main differences were in the iron, silicon and carbon contents, in good agreement with the different dilutions in the samples. The grey cast iron shows flakes of graphite evenly distributed in a ferritic matrix .

As it would be expected, the increase in the weld current and, therefore, increase in dilution, gives rise to a decrease of the hardness either in the coating, undesirable in terms of wear, or in the heat affected zone (HAZ), which is favourable for the toughness of this zone. The average surface hardness of coatings C100, C140 and of grey cast iron was 300, 195 and 150 Vickers ($HV_{0.5}$), respectively. The detailed characterization of the microstructure of each coating and the hardness variations with increasing dilution can be found in our previous publication [11].

4. Tribological behaviour of coatings

4.1. Wear rate

Figure 2 shows the wear loss rate of coatings and grey cast iron tested at different temperatures. It clearly shows that at room temperature the wear loss of coatings and grey cast iron is very low, and almost independent of the substrate dilution. C100 coating displays a little higher wear resistance than C140 coating, in agreement with its higher hardness. The observed similar level of wear rate of the grey cast iron as compared to the Ni coatings at RT is due to its higher amount of graphite, that can act as solid lubricant, leading to a less volume loss of material, compensating its lower hardness [13, 14].

At temperature of 550 ºC an abrupt increase of the wear rate of the coatings was observed; however, it dropped for 700 ºC. The first increase of the wear rate can be

attributed to the spontaneous oxidation, while, as it will be discussed later, the following decrease at 700 ºC could be related to the formation of a thick layer of oxides on the wear track preventing further wear of the coatings. Besides, the coating produced with high dilution displayed much higher wear resistance at elevated temperatures than C100 coating. This behaviour is a result of the easier oxidation of C140 coating that will contribute to the formation of a high amount of protective oxides in the contact zone.

For the grey cast iron, a continuous increase of the wear rate with increasing temperature was observed, globally with much higher wear rate than the Ni-based coatings. This is an expected result since a rapid loss of the material mechanical strength and an increasing oxidation rate with temperature are typical of grey cast iron.

4.2. Friction coefficient

The evolution of the friction coefficient of the coatings and grey cast iron with increasing testing temperature is shown in Figure 3. As expected, all the friction curves displayed two distinct regions: running-in and steady state stages. At RT, the running-in is similar for both Ni-based coatings and characterized by a strong increase of the friction coefficient to the highest value of 0.74, followed by a rapid decrease down to 0.41, after the first 1000 laps. On the other hand, in grey cast iron, the friction coefficient slightly increased over time reaching the steady state after 4000 laps with a friction coefficient of about 0.39. Grey cast iron exhibited relatively low friction coefficient at RT as compared to the Ni-based alloys, behaviour related to the presence of graphite on the worn surface as was referred to above.

A long running-in period with a progressive increase of the friction coefficient was also noticed for the grey cast iron at 550 ºC; however, the friction was much higher

suggesting different contact conditions. On the other hand, Ni-based coatings displayed very short running-in periods with the friction coefficient stabilized at similar values as in RT tests.

Finally, at 700 ºC different trends between cast iron and coatings were found. In the first case, the steady state is achieved almost immediately at a value much higher than the one at the running in period at 550 ºC, but ending with a smaller value in the final friction coefficient. For C100 and C140 coatings, after a long running in period, the friction stabilized at values of approximately 0.6 and 0.65, higher than those achieved at lower temperatures. Such trends suggest that different contact conditions should have taken place in both situations. In most of tribological tests, especially in those at high temperatures, the friction curves displayed quite unstable values. According to Kesavan and Kamaj [15], such behaviour demonstrates the presence of a tribolayer on the sliding surfaces which is continually worn out and re-formed again, resulting in short-term friction coefficient oscillations.

4.3. Wear mechanisms and surface analysis of coatings

The changes of the wear rates and friction coefficients described above can be attributed to a great number of factors related to the chemical composition, the physical properties of the materials, or the applied test conditions. Therefore, the investigation of the interaction between the specimen-counterpart pair was carried out. SEM-EDS and Raman spectroscopy were used to characterize the dominant wear mechanisms and the wear debris originated by the tribological testing.

4.3.1. Worn surfaces at room temperature

Typical SEM micrographs of the worn surface of the samples tested against Al_2O_3 balls at RT are depicted in Figure 4. The wear tracks of Ni-based coatings are similar; they present a rough morphology with evidence of tribo-oxidation. A discontinuous and cracked oxide adhered layer was formed on the surface, which reveals its brittle nature. Raman spectra performed at the oxidized worn surface (see spectra a) and b) in Fig. 5) confirmed the presence of the oxides and graphite, namely through the Raman active modes assigned to Ni-O [16] and C [17]; the latter almost inexistent in C100 sample spectrum as a consequence of its much lower dilution. These results are in good agreement to EDS analysis (see Fig. 5 a) for C100 coating), which showed essentially strong signals of Ni and O. Vestiges of Fe, Si, Al and C were also detected which indicated the presence of small amounts of Fe, Si and Al oxides, not detected by Raman spectroscopy possible due to either their small amounts or their placement within or below the Ni-O oxide layer. Similar wear debris was found on the wear scars of the balls too. During the wear tests the friction, generated by the sliding of the ball against the coating surface, causes the increase of the local temperature (flash contact temperature), mainly in the protuberances contact, promoting the tribo-oxidation of the surface. Due to the sliding movement, material from the ball, coating and oxides will spall off, generating free wear debris which will oxidize and adhere to the ball/coating surface, scratching the antagonist surface and promoting a continuous removal of the coating. In this stage, the amount of oxidized material will increase and, consequently, the contact between the ball and the non-oxidized coating surface progressively decreases. Further, due to the combined effect of contact pressure and brittle oxide, the transfer-layer will crack. With the test running, the oxide tribo-layer will grow and the

contact shall be governed by the compromise between the growing tribo-layer and its destruction and attachment to the counterpart, until a steady state will occur. An illustrative scheme of the oxide tribo-layer grows is shown in Figure 6. The contact between the non-oxidised coating and the ball gave rise to a high friction coefficient that should decrease with oxide formation, until a constant and lower value will be achieved. The same oxide, NiO as shown by Raman spectroscopy, is formed on the top surface in both coatings, explaining their similar levels of wear resistance and friction coefficient, despite of their discrepancies in chemical composition, microstructures and hardness, promoted by the different dilution levels. The high hardness of the metallic coatings, in conjunction with the protective effect of the hard NiO oxide, led to very low wear volumes.

Distinct wear behaviour was found for the grey cast iron. The wear track displays a very clean surface with fine scratches parallel to the relative sliding movement (suggesting abrasion wear mechanism) and some adherent wear debris. Furthermore, in some places black regions can be noticed, which can be attributed to either the presence of graphite flakes or their pull-out from the material [18]. EDS analysis performed at the wear debris revealed that they are formed by a mixture of original and oxidized material, including a weak signal from graphite lamellas. Similar phases were detected on the clean worn surface, although C peak was much more intense there. Raman spectroscopy analysis showed the presence of hematite (α-Fe_2O_3) [19] and graphite through the characteristic D and G bands [20] (see spectrum c) and d) of Fig. 5). During sliding experiments the movement of the ball promotes the wear of surface specimen with production of both oxide and graphite debris. Graphite will act as a solid lubricant in tribo-film, promoting a decrease of friction coefficient and having, indirectly, an important impact on reducing the wear [13, 14].

4.3.2. High Temperature

When sliding occurred at 550 ºC, C100 and C140 coatings also showed oxides on the contact surface. However, C140 wear track was almost fully covered whereas C100 exhibited an irregular surface with a mixture of clean wear zones and oxidized ones with signs of adhesive and abrasive wear (see Fig. 7 a-b), suggesting an incomplete formation of an oxide transfer layer. The difference between the two samples can be interpreted considering their oxidation behaviour. In fact, C100 sample oxidizes through the formation of a protective mixture of oxides based on B / Si over a Ni-based oxide layer [10]. Although these oxides are protective in static oxidation conditions, B-oxide melts below 600 ºC [21, 22], which leads to its easy removal hindering the formation of a stable oxide layer over the surface. As the process requires some time, since temperatures are still low being oxidation rates low [10], the destruction of the growing oxide layers is relatively easy and the formation of a transfer layer is limited due to the dragging effect caused by the ball sliding and melted B-oxide. Simultaneously, with the sliding movement asperities will break producing wear debris, which in the contact will promote the abrasion of both the ball and the coating. With test running, high amounts of coating material will be removed and/or oxidized. Therefore, high wear volumes are expected and indeed the steep increase in the wear rate can be noticed in Fig. 2. In the case of C140 sample, besides Ni-based oxides, iron oxide is also formed during oxidation at these temperatures [10]. The oxidation rates are much higher compared to C100 sample due to its higher dilution. Therefore, a higher amount of oxide debris can be produced facilitating the formation of a continuous oxide transfer layer. The surface is thus protected more quickly and, in spite of the much higher wear

rate in comparison to RT test, the wear resistance is higher than that for C100 sample. The growth of the oxide layer can, then, be attributed to: i) spontaneous oxidation of the coating at the testing temperature before test starting and ii) debris produced from the fracture of the asperities that more easily oxidize due to the sliding movement.

Raman analysis performed at the adherent wear debris on C100 coating (see Figure 8) indicated that they were mainly formed by Ni-O although, according to the EDS analysis, Fe-O, Si-O and Al-O should also coexist in much less amount, in good agreement to our previous work on the oxidation behaviour of this coating [10]. At the clean zone (bottom part of the worn surface) EDS showed that it is non-oxidized coating material. For C140 coating, Raman analysis showed similar oxides but, in this case, a significant amount of iron oxides (hematite and magnetite (Fe_3O_4) were also detected, in good agreement to the higher level of dilution and to the oxidation studies where this oxide was found to be the main constituent of the oxide scale [10]. Additionally, strong signals of C-based phases were detected by EDS. The whole tribological process at 550 ºC is schematized in figure 9.

Grey cast iron was fully covered with an oxide layer at this temperature, with scratches parallel to the movement of the sliding. The main oxides identified in the wear track were hematite and magnetite (see Raman spectrum c) of Figure 8). The softening of the material, induced by the temperature increase, together with the total depletion of graphite from the track surface justify the sharp increase in the wear rate, as well as the increase in the friction coefficient in comparison to results at RT.

At 700 ºC the oxidation rate of Ni-based coatings increased significantly allowing rapid and easy formation of a continuous oxide layer on the worn surfaces (see Fig. 10). The oxide acts as a protective layer decreasing the wear loss of the coatings. As the major wear volume loss is produced during the formation of the protective oxide

layer, faster production of tribolayer decreased the wear rate in relation to 550 ºC testing (see Fig. 2). Similar results were achieved and in detail explained by Kesavan et al. [15]. Furthermore, since the oxidation rate of C140 coating is higher than that of C100 coating, the latter will take more time to form the oxide layer generating a higher coating wear volume in the initial stage of the wear process. As a consequence, total wear rate after the test will be higher as well. Thus, the evolution of the transfer-layer grown in these cases is similar to that described for the coating produced with high dilution tested at 550 ºC (shown in Figure 9 b)), but with a fast growth of the oxide scale. Raman analysis of the wear tracks of both coatings showed the presence of Ni-O (see spectra a) and b) of Fig. 11); moreover, iron oxides were identified in C140 coating.

On the other hand, grey cast iron oxidizes easily but the oxide does not support the sliding process and does not protect efficiently the base material. The increase in the temperature promotes a severe softening of the material and a high oxidation rate leading to a strong abrasion and, therefore, a very high wear loss. Raman analysis confirms the extensive formation of hematite in the wear track (spectra c of Fig. 11); signs of magnetite were also detected.

In summary, although dilution reduces the hardness of coatings, it has beneficial effect at high temperature tribological behaviour due to the faster formation of oxide layers (owing to its lower oxidation resistance) which protect the coating surface against wear.

Conclusions

Nickel based hardfaced coatings, deposited by plasma transferred arc on grey cast iron with two dissimilar levels of dilution, were tribologically tested at room and high temperatures and compared to uncoated grey iron. The results showed that the wear loss of the coatings was independent of the substrate dilution at room temperature; tribo-oxidation was the main wear mechanism. Despite its lower hardness, grey cast iron showed similar wear rate as Ni-based coatings due to the lubricious effect of a C tribo-layer formed on the sliding surfaces. Increase sliding test temperature to 550 ºC led to an abrupt increase of the wear rate of the coatings and the grey cast iron due to material softening and oxidation. Grey cast iron showed extremely high wear values due to the continuous removal of the oxides, which exposed the soft non-oxidized material. Ni-O based layer protected more efficiently the Ni-based coatings. Further increase in test temperature to 700 ºC led to the improvement of the wear resistance of the coatings and an intensification of the wear on grey cast iron. The coating produced with the highest dilution displayed the highest wear resistance at elevated temperatures. This behaviour was related to its lower oxidation resistance, which promoted the easier formation of high amounts of oxide wear debris and their agglomeration into compact oxide tribolayer acting as protection of wearing surfaces.

Acknowledgments

This research is sponsored by FEDER funds through the program COMPETE – Programa Operacional Factores de Competitividade – and by national funds through FCT – Fundação para a Ciência e a Tecnologia –, under the projects PTDC/EME-TME/122116/2010, PEst-C/EME/UI0285/2013 and CENTRO -07-0224 -FEDER - 002001 (MT4MOBI), as well as the grant (SFRH/BD/68740/2010).

References

[1] M. Cingi, F. Arisoy, G. Başman, K. Şeşen, The effects of metallurgical structures of different alloyed glass mold cast irons on the mold performance, Mater. Lett., 55 (2002) 360-363.

[2] L. Luo, S. Liu, J. Li, W. Yucheng, Oxidation behavior of arc-sprayed FeMnCrAl/Cr_3C_2-Ni_9Al coatings deposited on low-carbon steel substrates, Surf. Coat. Technol., 205 (2011) 3411-3415.

[3] R. Vaßen, M.O. Jarligo, T. Steinke, D.E. Mack, D. Stöver, Overview on advanced thermal barrier coatings, Surf. Coat. Technol., 205 (2010) 938-942.

[4] A. Gatto, E. Bassoli, M. Fornari, Plasma Transferred Arc deposition of powdered high performances alloys: process parameters optimisation as a function of alloy and geometrical configuration, Surf. Coat. Technol., 187 (2004) 265-271.

[5] K. Siva, N. Murugan, R. Logesh, Optimization of weld bead geometry in plasma transferred arc hardfaced austenitic stainless steel plates using genetic algorithm, Int. J. Adv. Manuf. Technol., 41 (2009) 24-30.

[6] C. Guo, J. Zhou, J. Chen, J. Zhao, Y. Yu, H. Zhou, High temperature wear resistance of laser cladding NiCrBSi and NiCrBSi/WC-Ni composite coatings, Wear, 270 (2011) 492-498.

[7] K. Gurumoorthy, M. Kamaraj, K.P. Rao, A.S. Rao, S. Venugopal, Microstructural aspects of plasma transferred arc surfaced Ni-based hardfacing alloy, Materials Science and Engineering: A, 456 (2007) 11-19.

[8] W. Li, Y. Li, C. Sun, Z. Hu, T. Liang, W. Lai, Microstructural characteristics and degradation mechanism of the NiCrAlY/CrN/DSM11 system during thermal exposure at 1100 ^{0}C, J. Alloys Compd., 506 (2010) 77-84.

[9] V. Balasubramanian, A.K. Lakshminarayanan, R. Varahamoorthy, S. Babu, Application of Response Surface Methodolody to Prediction of Dilution in Plasma

Transferred Arc Hardfacing of Stainless Steel on Carbon Steel, J. Iron. Steel Res. Int., 16 (2009) 44-53.

[10] F. Fernandes, A. Cavaleiro, A. Loureiro, Oxidation behavior of Ni-based coatings deposited by PTA on gray cast iron, Surf. Coat. Technol., 207 (2012) 196-203.

[11] F. Fernandes, B. Lopes, A. Cavaleiro, A. Ramalho, A. Loureiro, Effect of arc current on microstructure and wear characteristics of a Ni-based coating deposited by PTA on gray cast iron, Surf. Coat. Technol., 205 (2011) 4094-4106.

[12] F. Fernandes, A. Ramalho, A. Loureiro, A. Cavaleiro, Wear resistance of a nickel-based coating deposited by PTA on grey cast iron, Int. J. Surf. Sci. Eng., 6 (2012) 201-213.

[13] A. Vadiraj, G. Balachandran, M. Kamaraj, B. Gopalakrishna, D. Venkateshwara Rao, Wear behavior of alloyed hypereutectic gray cast iron, Tribology International, 43 (2010) 647-653.

[14] B.K. Prasad, Sliding wear response of a grey cast iron: Effects of some experimental parameters, Tribology International, 44 (2011) 660-667.

[15] D. Kesavan, M. Kamaraj, The microstructure and high temperature wear performance of a nickel base hardfaced coating, Surf. Coat. Technol., 204 (2010) 4034-4043.

[16] N. Mironova-Ulmane, A. Kuzmin, I. Steins, J. Grabis, I. Sildos, M. Pärs, Raman scattering in nanosized nickel oxide NiO, Journal of Physics: Conference Series, 93 (2007) 012039.

[17] S.-R. Jian, Y.-T. Chen, C.-F. Wang, H.-C. Wen, W.-M. Chiu, C.-S. Yang, The influences of H_2 plasma pretreatment on the growth of vertically aligned carbon nanotubes by microwave plasma chemical vapor deposition, Nanoscale Research Letters, 3 (2008) 230-235.

[18] S.N. Pandya, S.K. Nath, G.P. Chaudhary, Friction and wear characteristics of TIG processed surface modified grey cast iron, 1 (2009) 516-527.

[19] D.L.A. de Faria, S. Venâncio Silva, M.T. de Oliveira, Raman microspectroscopy of some iron oxides and oxyhydroxides, Journal of Raman Spectroscopy, 28 (1997) 873-878.

[20] A.C. Ferrari, J. Robertson, Raman spectroscopy of amorphous, nanostructured, diamond–like carbon, and nanodiamond, Philosophical Transactions of the Royal Society of London. Series A: Mathematical, Physical and Engineering Sciences, 362 (2004) 2477-2512.

[21] Y.Q. Li, T. Qiu, Oxidation behaviour of boron carbide powder, Materials Science and Engineering: A, 444 (2007) 184-191.

[22] V.A. Lavrenko, Y.G. Gogotsi, Influence of oxidation on the composition and structure of the surface layer of hot-pressed boron carbide, Oxid. Met., 29 (1988) 193-202.

Figure captions

Figure 1 – Optical micrograph of C100 coating.

Figure 2 – Variation of the wear rate of coatings and grey cast iron with test temperature.

Figure 3 – Friction coefficient evolution with increasing test temperature of: a) C100 coating, b) C140 coating, c) grey cast iron.

Figure 4 – SEM morphology in secondary electrons of worn surface of: a) C100 coating, b) 140 coating, c) cast iron; all tested at room temperature. d) SEM/EDS spectra of point 1 marked in Fig. 5 a). e) and f) wear track profiles of: C140 coating, and grey cast iron, respectively.

Figure 5 – Typical Raman spectra performed on the worn surface of: a) C100 coating tested at RT, b) C140 coating tested at RT, c-d) adherent wear debris and clean surface of grey cast iron, respectively, tested at room temperature.

Figure 6 – Evolution of the tribo-layer growth on the coatings tested at room temperature.

Figure 7 – SEM morphology in secondary and backscattered electrons of worn surface of: a-b) C100 coating, c-d) 140 coating, e-f) cast iron; all tested at 550 ºC.

Figure 8 - Raman spectra performed on the worn surface of: a) C100 coating tested at 550 ºC, b) C140 coating tested at 550 ºC, c) grey cast iron tested at 550 ºC.

Figure 9 - Evolution of the tribo-layer growth at 550 ºC on coatings: a) produced with low dilution, b) produced with high dilution.

Figure 10 – SEM morphology in secondary and backscattered electrons of worn surface of: a-b) C100 coating, c-d) 140 coating, e-f) cast iron; all tested at 700 ºC.

Figure 11 - Raman spectra performed on the worn surface of: a) C100 coating tested at 700 ºC, b) C140 coating tested at 700 ºC, c) grey cast iron tested at 700 ºC.

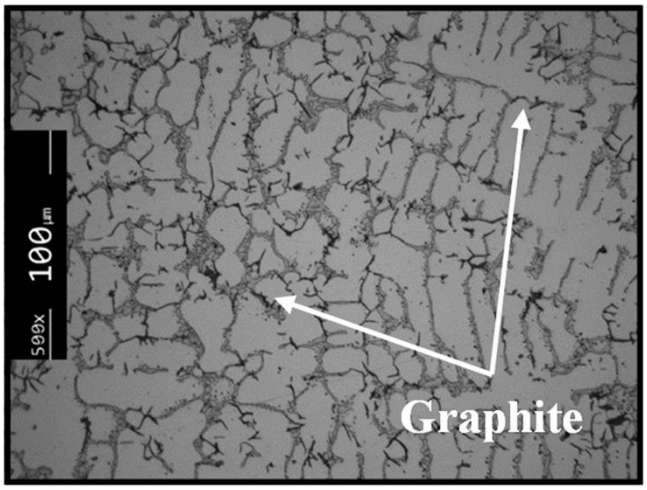

Fig. 1

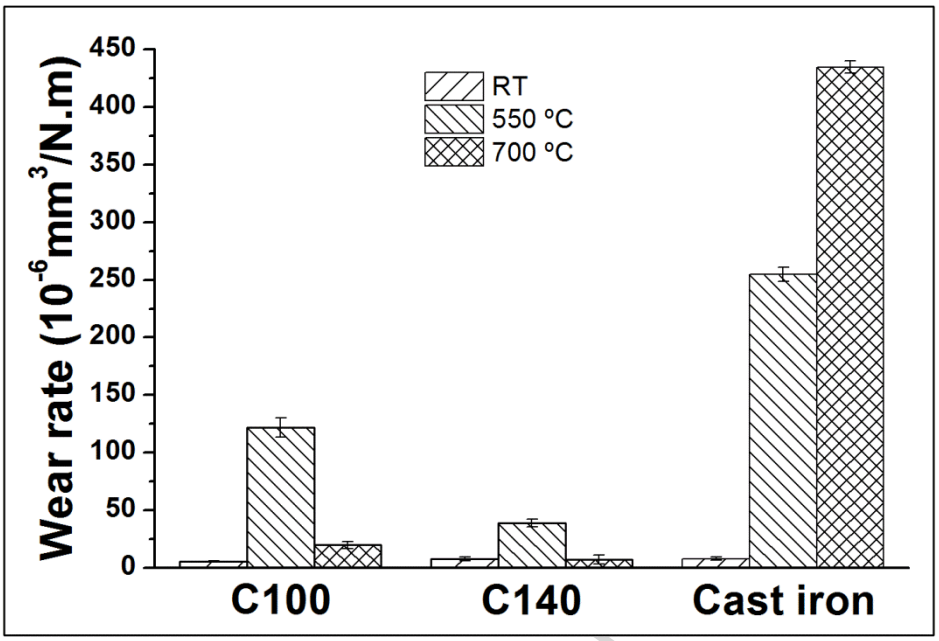

Fig. 2

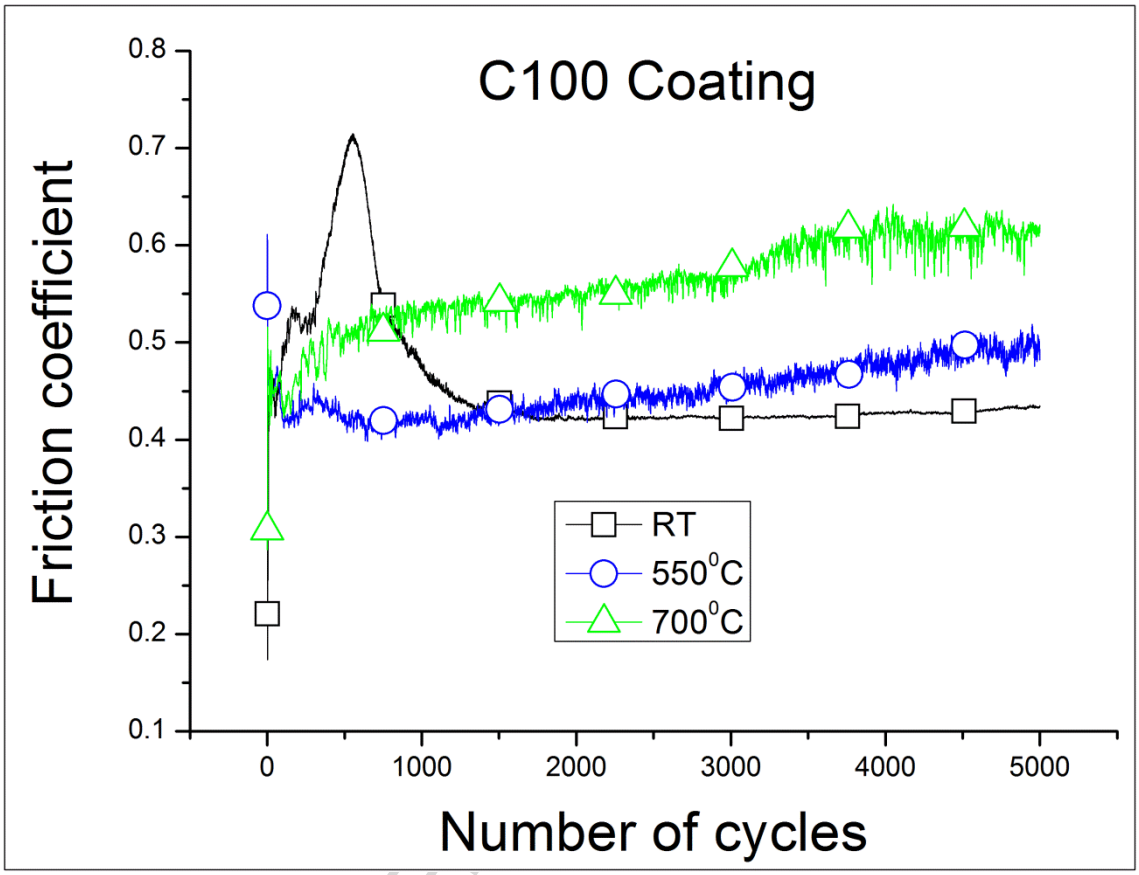

Fig. 3a

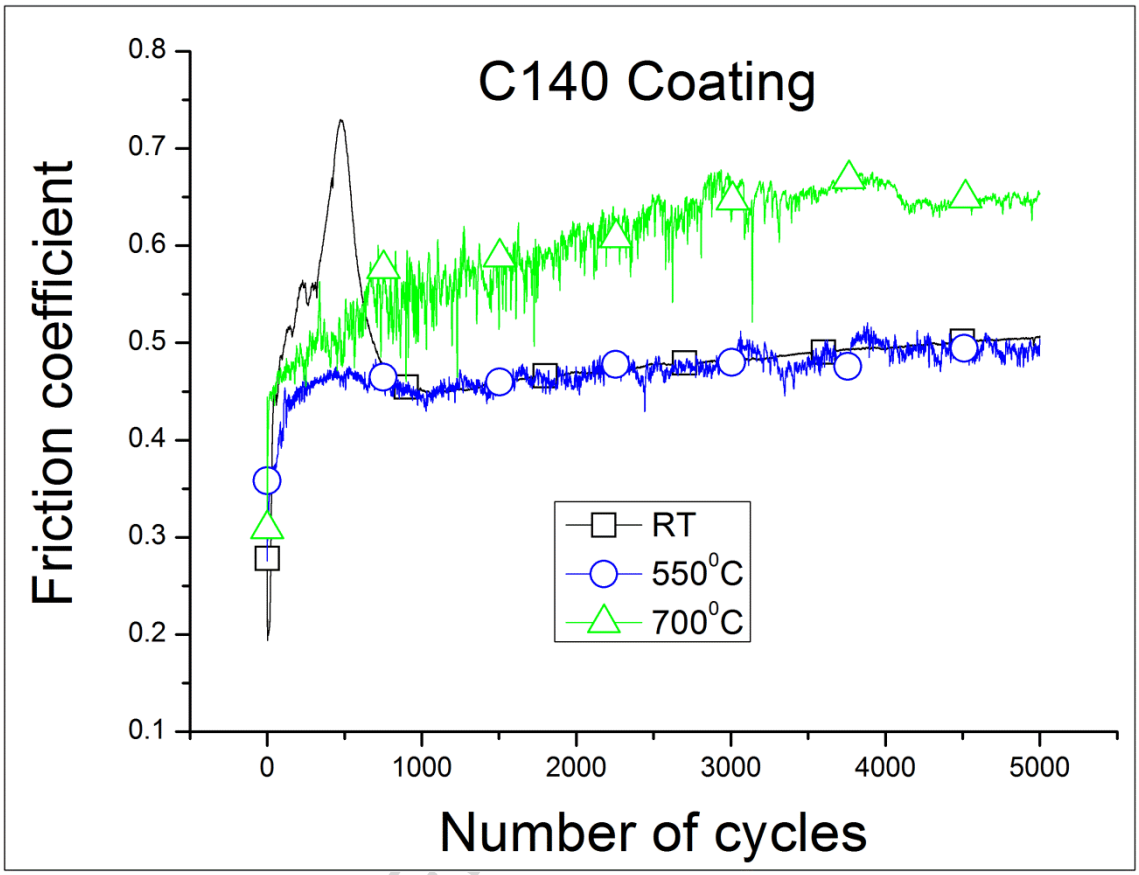

Fig. 3b

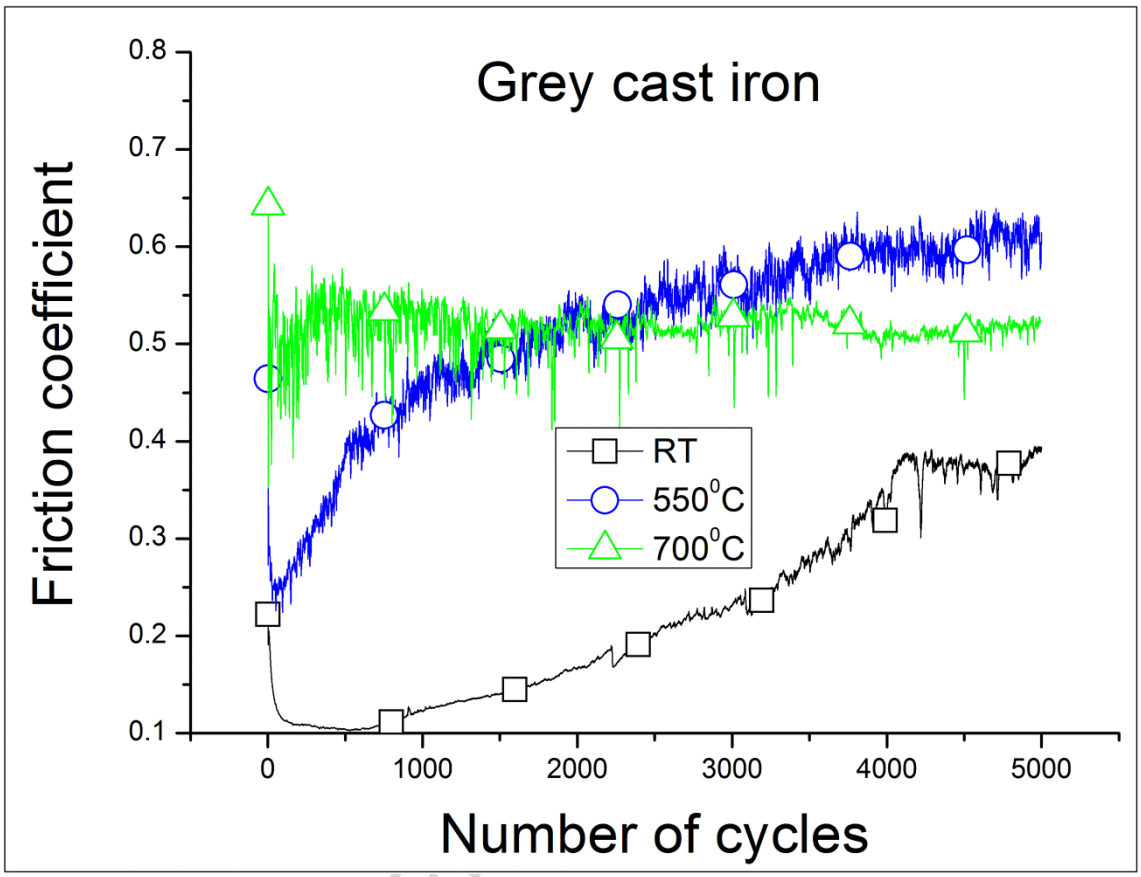

Fig. 3c

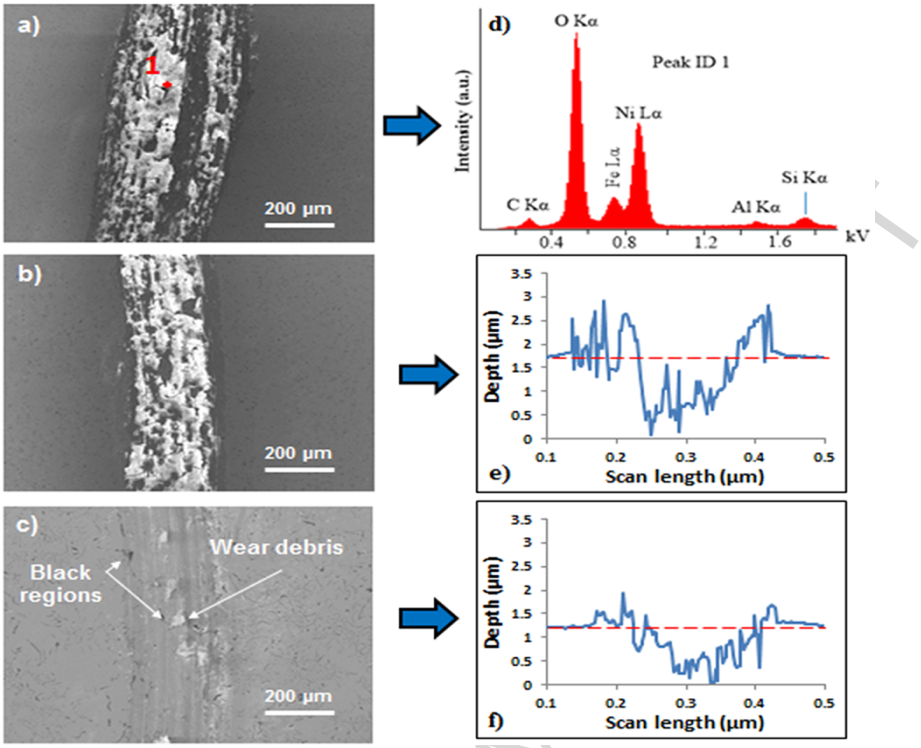

Fig. 4

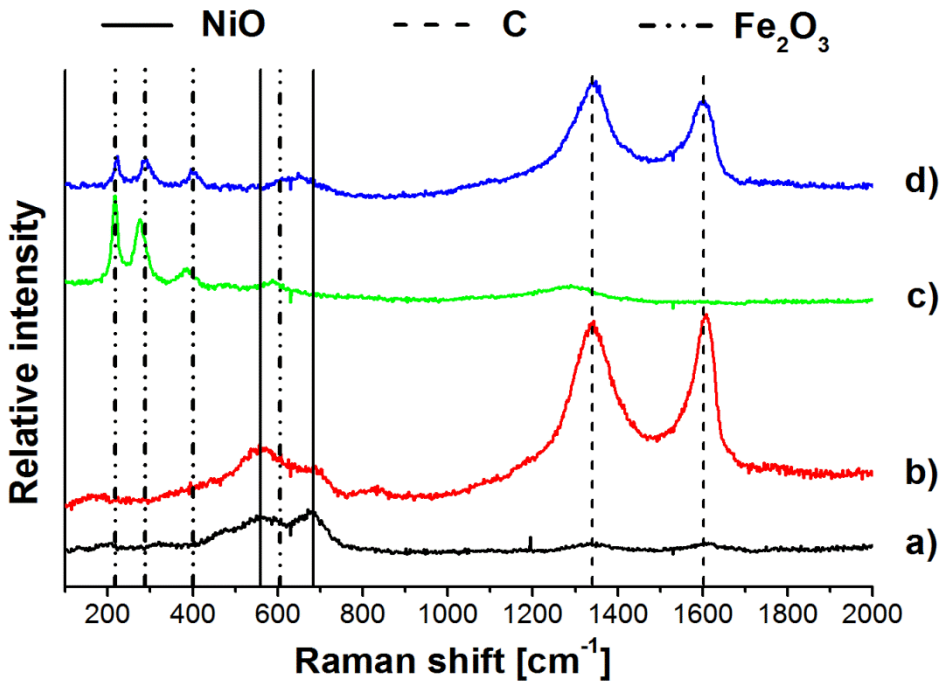

Fig. 5

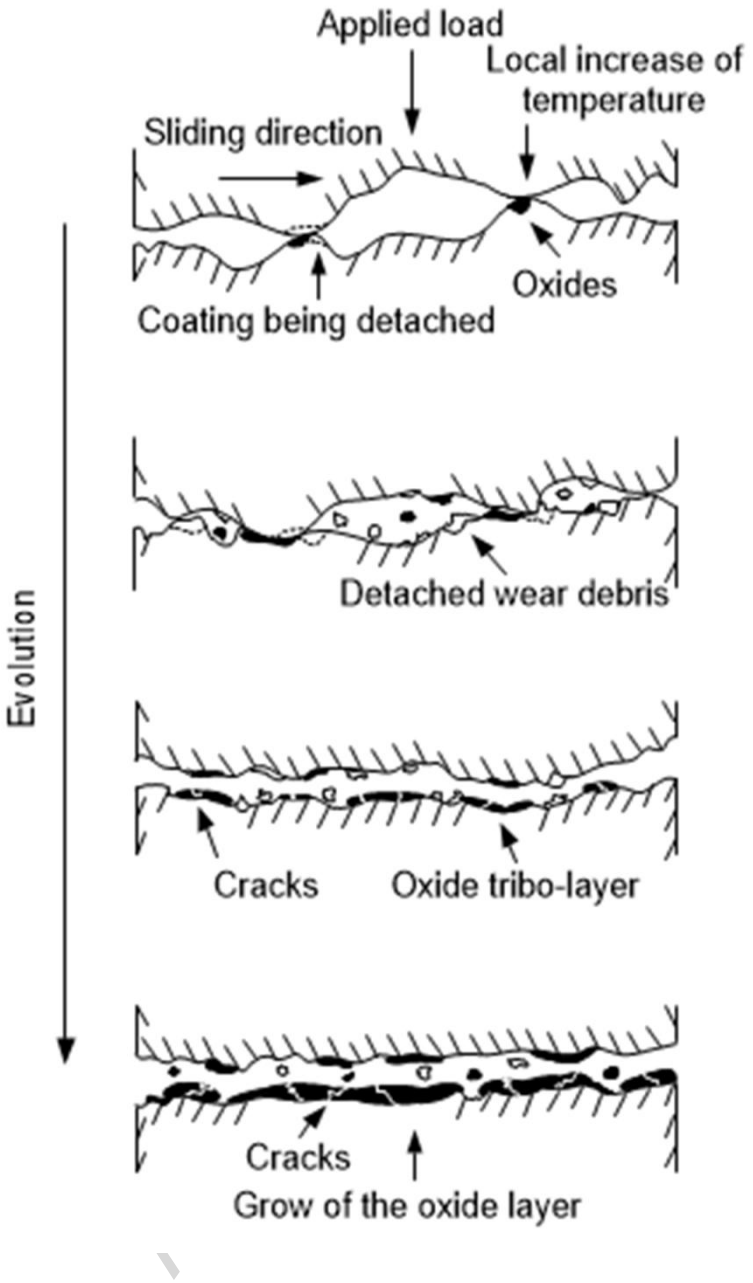

Fig. 6

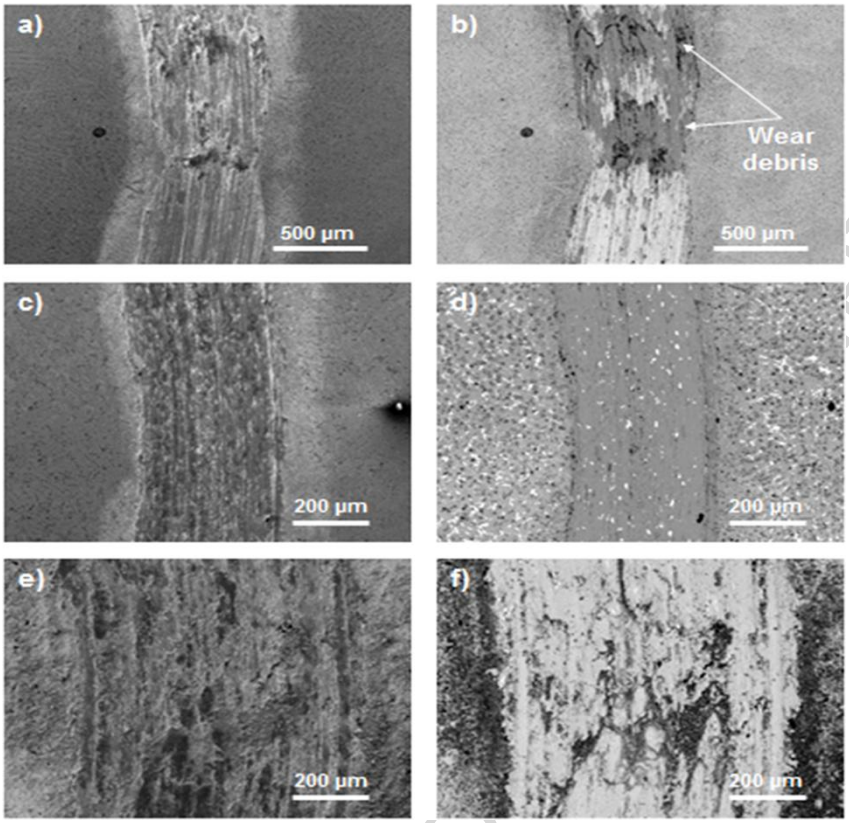

Fig. 7

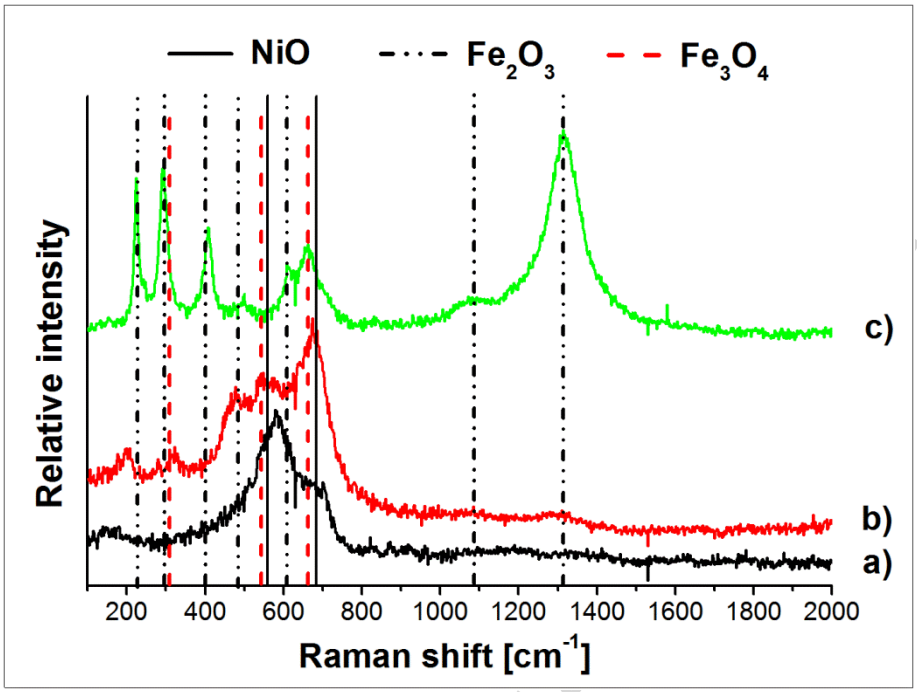

Fig. 8

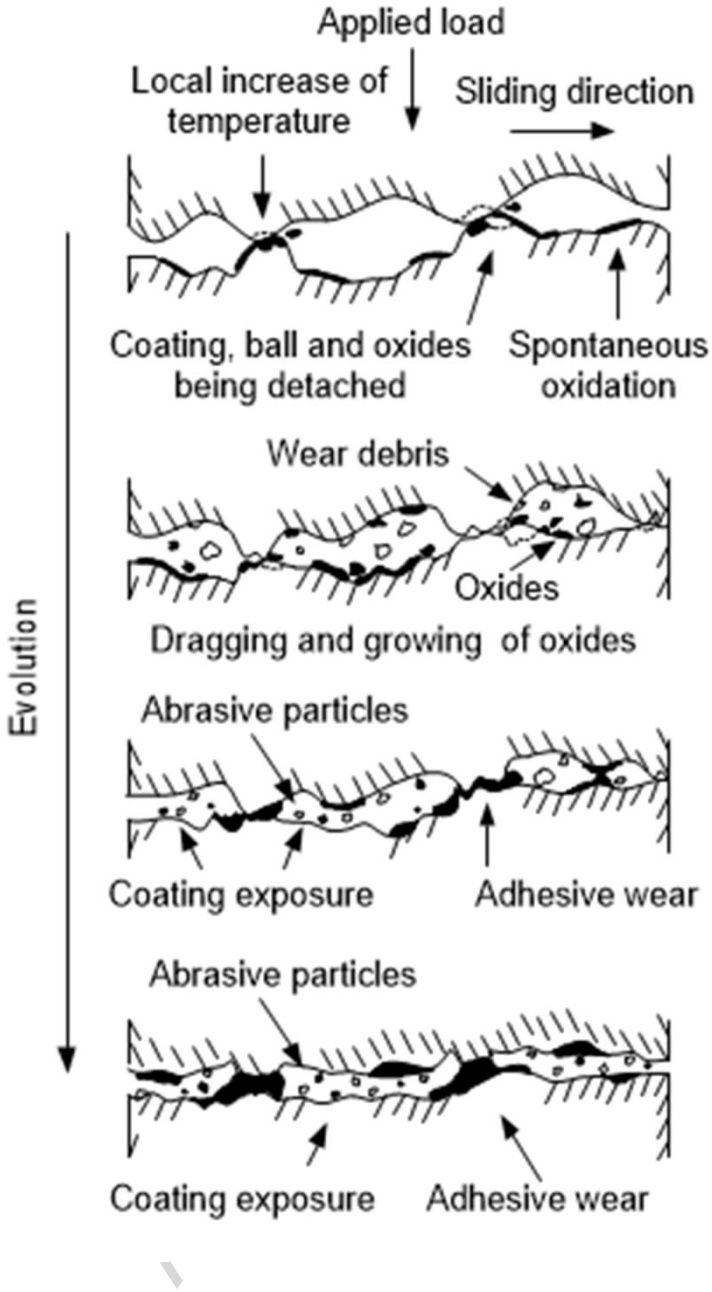

Fig. 9a

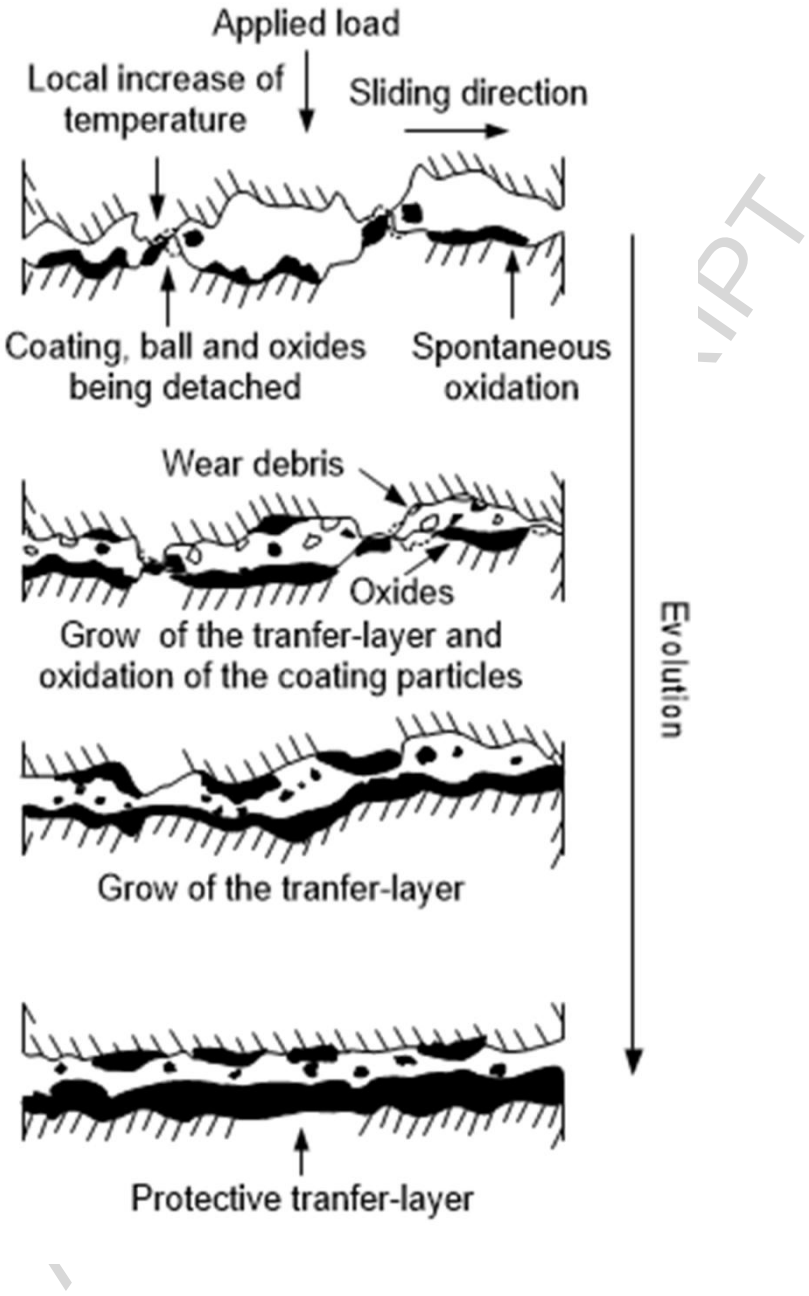

Fig. 9b

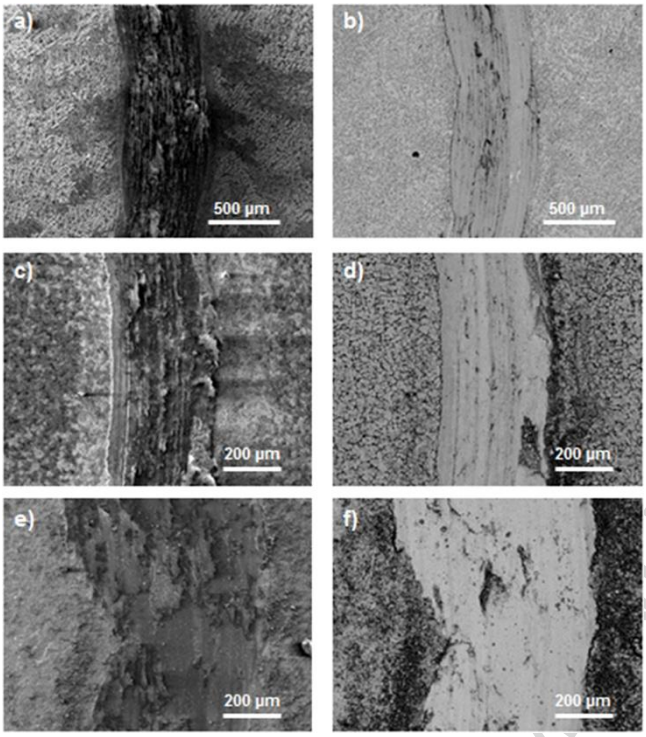

Fig. 10

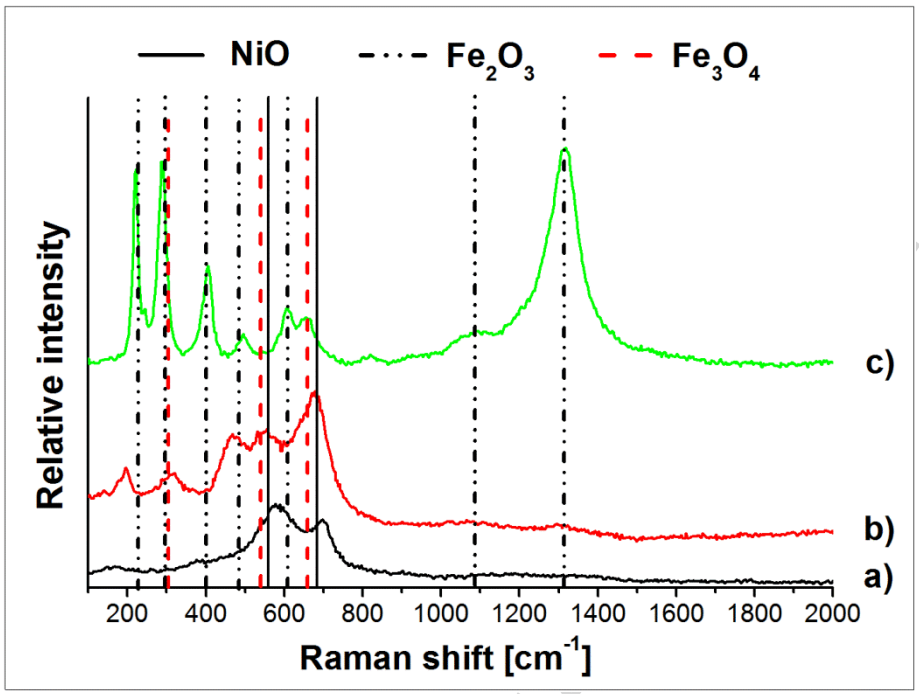

Fig. 11

Table 1 – Main deposition parameters.

	Main arc current (A)	Powder feed rate (rpm)	Travel speed (mm/s)	Powder feed gas flow rate (l/min)	Plasma gas flow rate (l/min)	Shielding gas flow rate (l/min)	Torch work distance (mm)	Oscillation (mm)	Preheat temperature ºC
C100	100	20	2	2	2.2	20	13	4	480
C140	140	20	2	2	2.2	20	13	4	480

Table 2 - Nominal chemical composition (wt.%) of the grey cast iron and nickel-based alloy powder.

Base material	C	Mn	Si	P	S	Cr	Ni	Mo	V	Ti	Fe
Grey cast iron	3.60	0.60	2.00	< 0.20	< 0.04	< 0.20	<0.50	0.50	0.10	0.20	Balance
Hardfacing			C	Cr	Si	B	Fe	Al	F	Co	Ni
Ni-alloy			0.14	2.45	2.56	0.86	1.08	1.30	0.01	0.08	Balance

Table 3 - Nominal chemical composition (wt.%) of coatings evaluated by SEM-EDS.

	wt. % of elements					
Coating	Ni	Fe	C	Si	Al	Cr
C100	85.4	8.5	0.3	2.2	0.8	2.9
C140	55.7	37.7	1.3	2.5	0.6	2.2

Highlights

- At RT, the tribological performance of coatings is independent of the substrate dilution.
- Tribo-oxidation wear was identified on the wear track of coatings at RT.
- At high temperatures (HT), coating with high dilution performs better.
- Formation of a continuous and thick oxide tribo-layer was responsible for HT performance.